

Analysis of Forming Limits During Cold Forging of Aluminum Hybrid Billets



Karl C. Grötzinger, Roman Kulagin, Dmitry Gerasimov,
and Mathias Liewald

Abstract Metal forming processes for manufacture of hybrid components with complex geometry is one of the most promising trends in materials science. At the same time, such processes pose serious challenges regarding the interface properties between the different materials. Thus far, models are existing to describe cold welding of hybrid components and their plasticity during following deformation processes. However, these models have been developed and validated mainly for processes, where stress and strain states are recognized as simple (e.g., drawing, roll bonding). In this contribution, a flange upsetting process using hybrid billets made of AA-6060 and AA-7075 is subjected, where the deformation conditions significantly differ (non-monotonous and complex strain history). The main aim of this paper is to investigate such process with special emphasis on acting stress conditions in the interface with respect to delamination effects occurring during cold forging experiments. Also, the influence of an initial bond between the aluminum components, created by compound hot extrusion, is investigated both experimentally and numerically. In this context, three geometrical models of the hybrid billet (variation of diameter and wall thickness of the reinforcing component) were used. Analyses show that even if bonding in extrusion process is not ideal and depends on various influencing parameters, it makes subsequent cold forging process more stable and reliable regarding material flow compared to billets without initial bond.

Keywords Hybrid materials · Cold forging · Numerical simulation

K. C. Grötzinger (✉) · M. Liewald
Institute for Metal Forming Technology, University of Stuttgart, Holzgartenstr. 17, 70174
Stuttgart, Germany
e-mail: karl.groetzinger@ifu.uni-stuttgart.de

R. Kulagin
Institute of Nanotechnology (INT), Karlsruhe Institute of Technology,
Hermann-Von-Helmholtz-Platz 1, 76344 Eggenstein-Leopoldshafen, Germany

D. Gerasimov
Micas Simulations, Temple Court, 107 Oxford Road, Oxford OX4 2ER, UK

© The Rightsholder, under exclusive licence to [Springer Nature Switzerland AG], part
of Springer Nature 2024

J. Kusiak et al. (eds.), *Numerical Methods in Industrial Forming Processes*, Lecture
Notes in Mechanical Engineering, https://doi.org/10.1007/978-3-031-58006-2_29

1 Introduction

The manufacture of hybrid components by metal forming poses serious challenges to process design and thus pre-determines numerous decisive trends in materials science [1]. Such components allow for combining of different materials to achieve a significant potential for lightweight design and integration of special functions. The property of the individual, separate parts that make up the hybrid, differs from the one of the joined assembly. Joining by forming therefore increases productivity and makes additional joining processes and connecting elements needless. As a result, energy and material can be used more efficiently. There are, however, several challenges to produce hybrid components, such as the inevitable presence of an interface between the parts, where property gradients and thus stress peaks are prevailing. Various process routes for the manufacture of hybrid components of different shape, such as sheet and bulk material, have been focused in literature. Cold forging is one such process for joining two or more components by forming [2]. The joining principle between involved components can be either a form fit, force fit or even a metal bond [3]. Comprehensive studies on the influence of component geometry on the interfacial contact during upsetting of bi-metallic billets were shown in [4]. In recent times, analytical approaches for estimating process load in hybrid forming processes were developed [5]. The kind of joint being created during deformation highly depends on the billet preparation, such as surface treatment, roughness, tolerances, and surface expansion in the interface exposed to prevailing normal and shear stresses [6]. Joining processes by cold forging of tubular components, however, pose several challenges such as buckling and contact loss as described in [4]. To overcome these challenges, the use of a two-step sequence seems promising: A first process includes the manufacture of the hybrid billet by extrusion, and a second one targets the deformation of component by cold forging. Such process route, as subjected in this publication, at first was introduced in [7]. It consists of a compound hot extrusion process of AA-6060 aluminum alloy featuring a continuously embedded tubular reinforcing component consisting of AA-7075.

In this publication, a comparison between different initial bond characteristics (unbond and bonded by compound hot extrusion) and their effect on subsequent cold flange upsetting process is subjected. Especially the stress distribution internally in the workpiece volume during flange upsetting process and suitable modeling of different bond characteristics belong to the main challenges in terms of estimating process limits. Cold flange upsetting in this study is investigated experimentally and numerically using three different geometrical billet variations. Gained results show that a certain initial bond, created by compound extrusion, leads to more stable process conditions and higher possible deformation in cold forging prior to delamination. Process simulations including stress analyses for different billet configurations were performed using QForm UK 10.2.4 commercial FE code. An approach for modeling opening and closing voids emerging in the interstice between both components is presented objecting a qualitative prediction of delamination effects during cold flange upsetting of extruded billets.

2 Materials and Methods

2.1 System Description

Compound hot extrusion, performed by the project partner Institute for Metal Forming and Lightweight Technology (IUL) Dortmund, was used to manufacture a hybrid aluminum extrudate (\varnothing 20 mm). Extruded hybrid rod consisted of a matrix from AA-6060 with a tubular reinforcing element from AA-7075 (see Fig. 1a). An extrusion ratio $R = 10.9$ was realized for the compound extrusion process to create hybrids with different inner diameter d_i and outer diameter d_a as depicted in Fig. 1c. The dimensions of the billet components prior to extrusion were chosen in such a way, that the process was feasible without fracture of the tubular reinforcing element. Main reason for choosing mentioned hot extrusion process parameters was to create a proper metal bond between the hybrid components during extrusion. For subsequent cold forging process, billets were cut from the continuous hybrid extrudate (length L_0 , diameter d_0). Cold flange upsetting was chosen as a suitable process as it poses challenges to the bond between the materials during deformation. Depending on the diameter ratio \bar{d}_i and \bar{d}_a of the three different reinforcing element dimensions I-III, particular stress conditions are prevailing, that provoke delamination effects between the material layers.

As shown in literature, compound hot extrusion may result into metallic bond between the components [8]. Qualitative estimation of bond strength for such process was performed in [9]. Numerical modeling of the compound extrusion process showed large deformation (effective strain up to $\varepsilon_{eff} = 3$) in the interface between

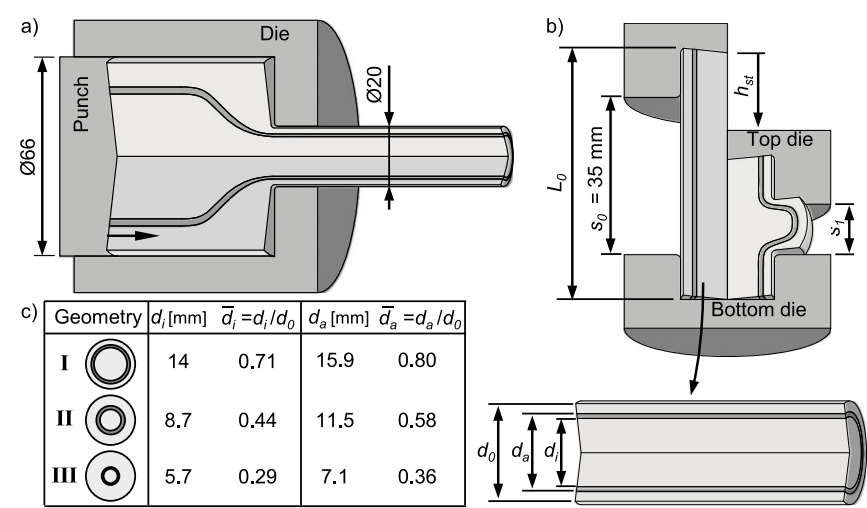


Fig. 1 a Compound hot extrusion, b cold flange upsetting, c billet dimensions

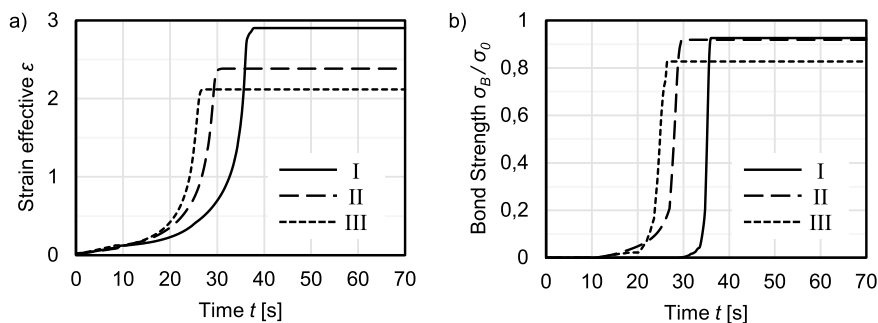


Fig. 2 Process parameters during compound hot extrusion **a** effective strain **b** relative bond strength according to Bay welding model [10]

the components and thus can lead to a metal bond due to the resulting high surface exposure in combination with the hydrostatic pressure during extrusion.

A qualitative bond strength calculation was examined using the Bay pressure welding criterion as published in [10]. Bond strengths for the three different geometrical variants I-III are depicted in Fig. 2b. Geometrical changes of the reinforcing element position lead to bond strength variations. For further effect analysis of bond characteristics on subsequent cold flange upsetting, billets with a clearance fit between the components were prepared by machining process.

2.2 Experimental Investigations

The billets for subsequent cold flange upsetting process were prepared using two different processing methods leading to different interface characteristics between the aluminum alloys. To investigate the effect of a clearance fit between the components and thus no bonding ($\sigma_B = 0$), samples were machined from round bars featuring a diametral clearance of 0.09 mm between the corresponding inner and outer part, see Fig. 3a. After machining, the three parts, consisting of core, tube, and shell, were manually assembled to make up the hybrid billet for cold forging. The hybrid billets with a certain bond due to compound hot extrusion process (assuming $\sigma_B \sim 1$) were cut from the hybrid extrudate as shown in Fig. 3b.

After the manufacturing process, the billets had been annealed, maintaining a holding time $t = 90$ min at $T = 380$ °C, followed by controlled cooling with a rate of 30 K/s down to $T = 250$ °C. Lubricant zinc stearate was applied in a tumbling process with a specific mass of 5.4 g/m² on the billet surface. Cold flange upsetting tests were performed on a 1000 kN hydraulic programmable press with position control featuring a ram speed of 10 mm/s. The experimental setup and the tool rack are shown in Fig. 4a. During forming tests, both tool load and ram position were measured in order to investigate the critical upsetting deformation, by which delamination effects between the material layers initially occur. The upsetting deformation is defined by φ

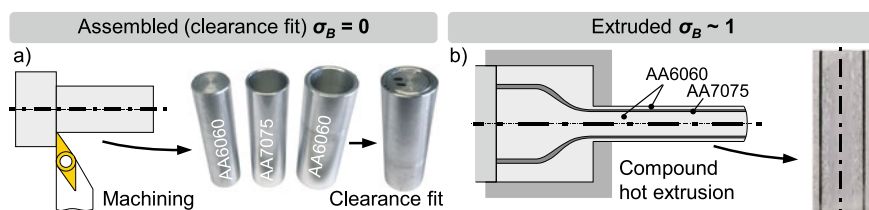


Fig. 3 Billet preparation by **a** machining with clearance fit and **b** extrusion with bonding

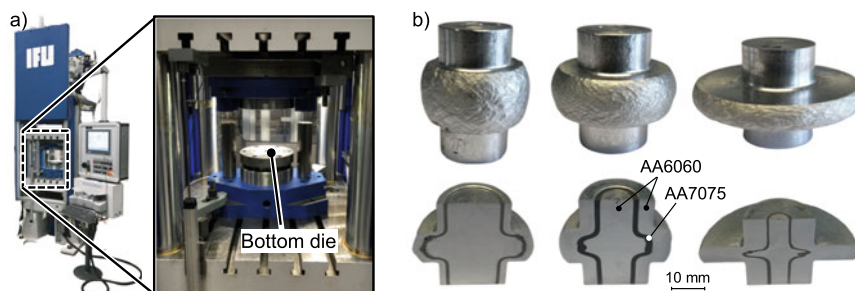


Fig. 4 Experimental setup for cold flange upsetting **a** hydraulic programmable press, **b** deformed hybrid components before and after cutting and etching

$= \ln(s_0/s_1)$, where $s_0 = 35$ mm is the initial distance between the dies and s_1 the final flange height at the end of the process according to the schematic in Fig. 1b. Delamination effects were detected by means of microscope analysis in the cross sections of the considered flange component. For better visibility of different alloys, sodium hydroxide was used to make the AA-7075 component appear in dark color, see Fig. 4b.

2.3 Numerical Investigation of Cold Flange Upsetting Using Hybrid Billets

Commercial FE code QForm UK 10.2.4 was used for numerical modeling of hybrid cold flange upsetting process. A 2D axisymmetric model with plastic workpiece definition and rigid tools was created. Initial workpiece temperature was 20 °C. Material characterization tests for both AA-6060 and AA-7075 in soft annealed state were conducted on a thermomechanical testing system Gleeble 3800 C in a temperature range of $20\text{ °C} \leq T \leq 200\text{ °C}$ applying strain rates between $0.1\text{ s}^{-1} \leq \dot{\varphi} \leq 10\text{ s}^{-1}$. The resulting flow curves for AA-6060 are depicted in Fig. 5a and for AA-7075 in Fig. 5b.

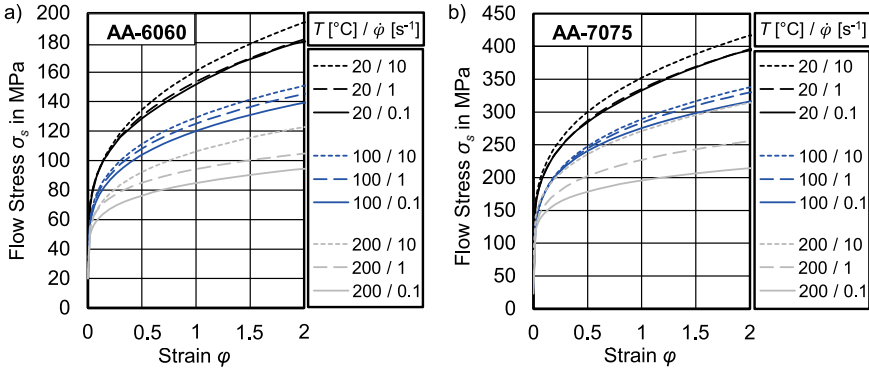


Fig. 5 Flow curves of **a** AA-6060 and **b** AA-7075 in annealed state based on table function

For the two proposed billet variants ($\sigma_B = 0$ and $\sigma_B \sim 1$), different modeling approaches available in QForm UK 10.2.4 were applied. In case of billets with clearance fit ($\sigma_B = 0$), a three-body design with interface contact definition showed similar deformation behavior as to experiments (see Fig. 6a). Friction factor $m = 0.4$ according to shear friction model in the FE code was used to define prevailing contact between the single workpiece bodies, where separation between the surfaces was allowed. Flange deformation geometry and process force were used to identify a suitable friction coefficient between tools and workpiece of $m = 0.6$. Top die velocity was set to 10 mm/s and heat transfer coefficient between workpiece and tools was defined to 30,000 W/(m²K).

In case of an initial bond between the workpieces due to billet manufacture by composite hot extrusion ($\sigma_B \sim 1$), a one-body model featuring local areas with different material properties was suitable (see Fig. 6b). As a result, one homogeneous calculation mesh was used and contact definition between the area of different material properties was neglected. The comparison between simulation and experiments resulted in friction factor $m = 0.3$ in the interface of tool and workpiece. Point tracking as well as subroutines were used to gain the required components of stress tensor in the interface area of the hybrid for further analysis.

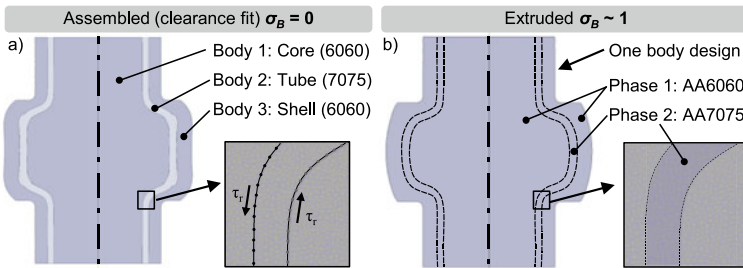


Fig. 6 Simulation models for **a** no initial bond between components **b** extruded billet

3 Results and Discussion

3.1 Experimental Results

Representative cross sections of all three geometry variants I-III and for both billet conditions ($\sigma_B = 0$ and $\sigma_B \sim 1$) are depicted in Fig. 7 as an axisymmetric view with a magnification next to the corresponding image. For each of the variants, multiple tests were conducted by increasing ram stroke and thus by decreasing flange height s_I , which is shown here by the upsetting logarithmic strain $\varphi = \ln(s_0/s_I)$. In case of billets with a clearance fit ($\sigma_B = 0$), an undefined and irregular deformation of the tubular reinforcing component made of AA-7075 was observed for multiple repetitions. In fact, buckling occurred due to the clearance fit, which led eventually in some cases to vortex formation as can be seen for variants I and III. Obvious delamination, however, could be detected only for geometrical variants I and II, where the tubular reinforcing element remained under radial compression for variant III. In each case, delamination effects occurred on the outside boundary of the reinforcement.

For compound hot extruded billets ($\sigma_B \sim 1$), the deformation of reinforcing element was much more stable and homogeneous (no buckling, no vortex formation)

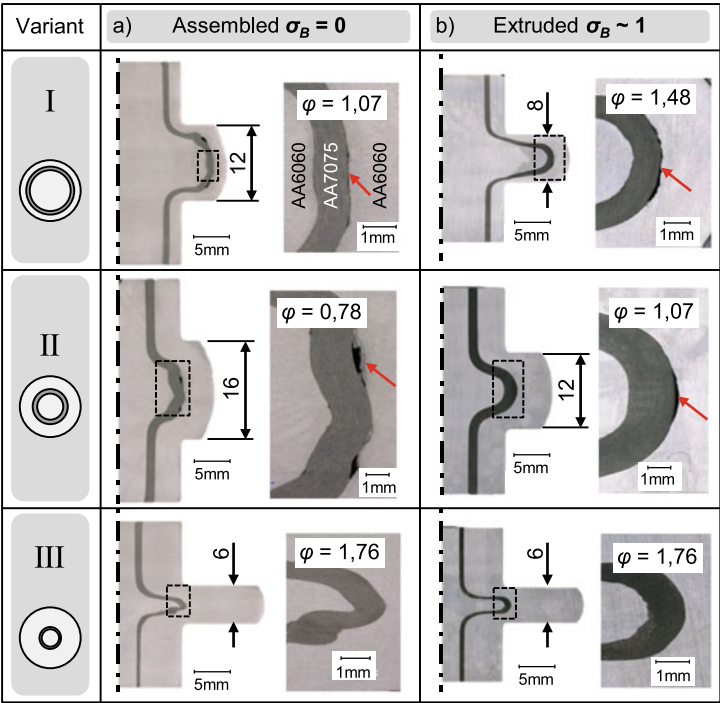


Fig. 7 Flange upsetting experimental results of different geometrical variants a without initial bond and b with extruded billets

than without bond. Regardless of which bond strength and which characteristics of bond actually prevailed in the extruded billets, bonding disclosed a positive effect on process stability and homogeneous strain distribution during cold flange upsetting. Also in this case, delamination effects appeared only at the outside boundary and if so, at approx. 35% higher deformation than without bond effect (see Fig. 7b, red arrows). For variant III, in both cases without bond and extruded billets, high deformations could be achieved without delamination effects.

3.2 Simulation Results

Numerical results according to the FE-model in Fig. 6a without initial bonding between the hybrid billet components are shown for the three geometry variants I-III and representative deformation states in Fig. 8. Radial stress σ_{xx} was used as a suitable state variable for analysis of possible bond detachment areas. For both variants I and II, experiments showed a noticeable separation between the outside shell and the reinforcing component at a certain amount of logarithmic strain. Using the proposed simulation model, loss of contact could be obtained in the outside boundary at similar deformation as to the experiment. Utilized simulation model, however, did not predict buckling of the reinforcing element as it could be obtained in experiments.

In case I, tensile radial stresses of approx. 30 MPa were detected close to the boundary in the outside shell from AA-6060, where detachment was actually prevailing also in experiments (see right column of first row in Fig. 8). When decreasing the outer diameter of the reinforcing component, the radial stress state close to the interface became more compressive. For geometry II, low compressive stress values had been calculated in the outer shell in the horizontal symmetry plane of the flange. Tensile radial stresses in the corners of the flange, together with the increased stiffness of the reinforcing element due to thick walls led to a visible loss of contact in the simulation model. Small outer diameter of reinforcement (III) resulted into a highly compressive radial stress state, which prevented delamination effects in both simulation and experiment.

Considering initial bonding between the billet components ($\sigma_B \sim 1$), the one-body simulation model presented in Fig. 6b showed areas with possible bond separation using the hydrostatic stress state. In both cases I and II, a positive hydrostatic stress state of approx. 25 MPa was obtained in the area of largest reinforcing element diameter, in which delamination also occurred in experiments. Considering geometry variant III with smallest outside diameter, more or less similar conditions were recognized as shown in Fig. 9, including large compressive hydrostatic stress level on the outside boundary, thus not allowing separation between the bodies.

Cold flange upsetting process showed highly non-monotonous stress profiles, which are depicted in Fig. 10 as triaxiality $\eta = \sigma_m / \sigma_{eff}$ over effective strain ε_{eff} , where σ_m is the hydrostatic stress and σ_{eff} effective stress. The triaxiality profiles were analyzed for two points P1 and P2 located representatively in the flange area, where delamination could be obtained in experiments. P1 (see Fig. 10a) was located

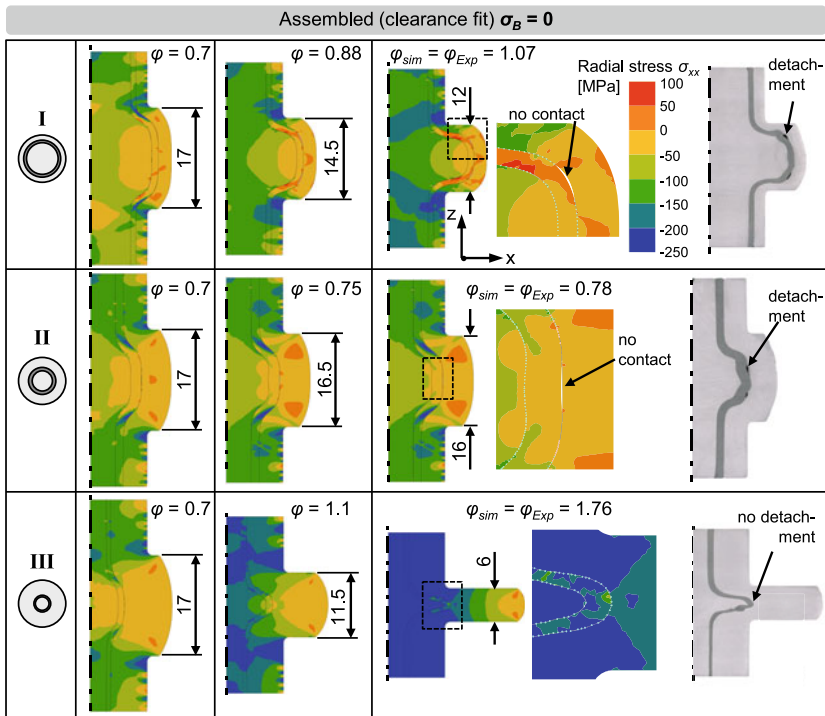


Fig. 8 Simulation results overview for different geometrical variants I-III with no initial bond between the materials $\sigma_B = 0$ for different deformation increments

at the corner of the bonding boundary in the transition zone towards the horizontal part of the reinforcing element and P2 was located right at the horizontal symmetry (see Fig. 10b). The characteristics in both points were similar, where geometrical variant III showed in each case negative stress triaxiality while variants I and II showed partly positive values. After a local maximum, triaxiality decrease could be obtained for all three variants. Due to the non-monotonous stress conditions in the interface, the porosity model, first introduced by Beygelzimer [11] was used to predict detachment of bond. The model describes porosity Θ as a function of triaxiality η , effective strain ε_{eff} and two constants A and B . Using this model, alternating triaxiality as present in this process, can be considered by increasing and decreasing porosity:

$$\frac{d\Theta}{d\varepsilon_{eff}} = A + B \times \Theta \frac{\sigma_m}{\sigma_{eff}} [11] \quad (1)$$

As thoroughly investigated in [11], the critical porosity to failure for several monolithic materials is $\Theta_{crit} \approx 1\%$. In a first approach of application, constants of this model were chosen to $A = 0.01$ and $B = 2.5$. The porosity calculation results for both points and all three geometrical variants are shown in Fig. 10c and d.

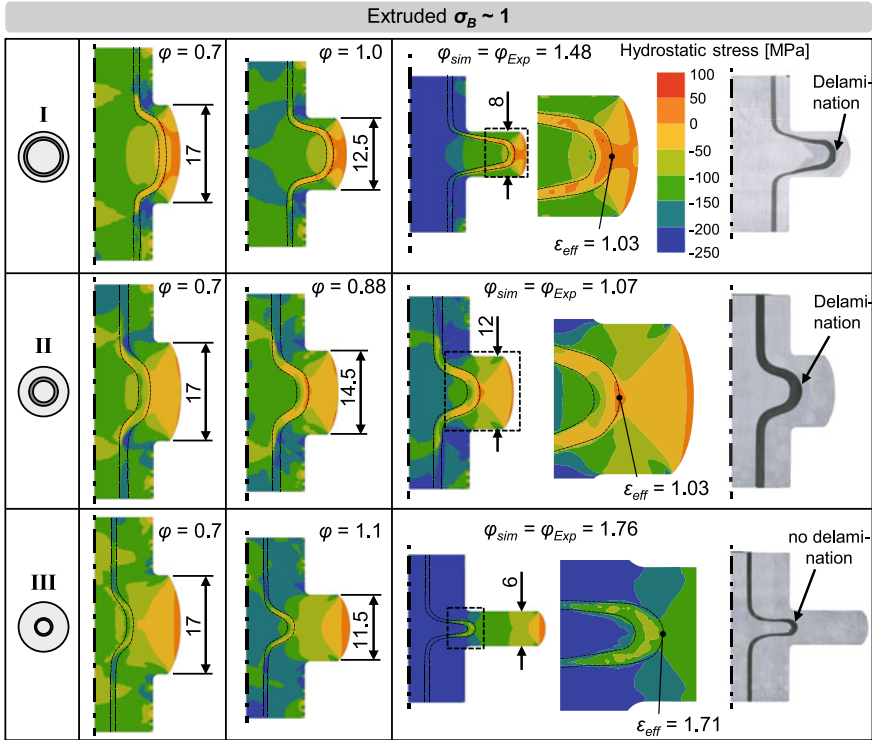


Fig. 9 Simulation results overview for different geometrical variants I-III with initial bond between the materials ($\sigma_B \sim 1$) for different deformation increments

For P1 and P2, observed tendencies appear comparable, so porosity was calculated for variant I to $\epsilon_{eff,I} (\Theta_{crit}) \approx 1.0$ and for variant II to $\epsilon_{eff,II} (\Theta_{crit}) \approx 1.2$. Variant III, however, did not exceed critical porosity value and even showed a decrease, which confirmed the finding of experiments as there was no detachment of bond found. Especially for P1 (see Fig. 10c), porosity decreased for all variants I-III, thus separation of interface was more likely to be reversed after certain degree of deformation. Comparing the critical effective strains $\epsilon_{eff,I} (\Theta_{crit})$ and $\epsilon_{eff,II} (\Theta_{crit})$ with the simulation results in Fig. 9, a good agreement could be found for variant I. For variant II, the strain to critical porosity was estimated approx. 16% higher than in experiments.

4 Summary and Conclusion

This study has shown that a certain bond strength between the components of a bi-metallic billet, manufactured by composite hot extrusion, in fact makes subsequent cold forging process more stable regarding material flow compared to billets, that

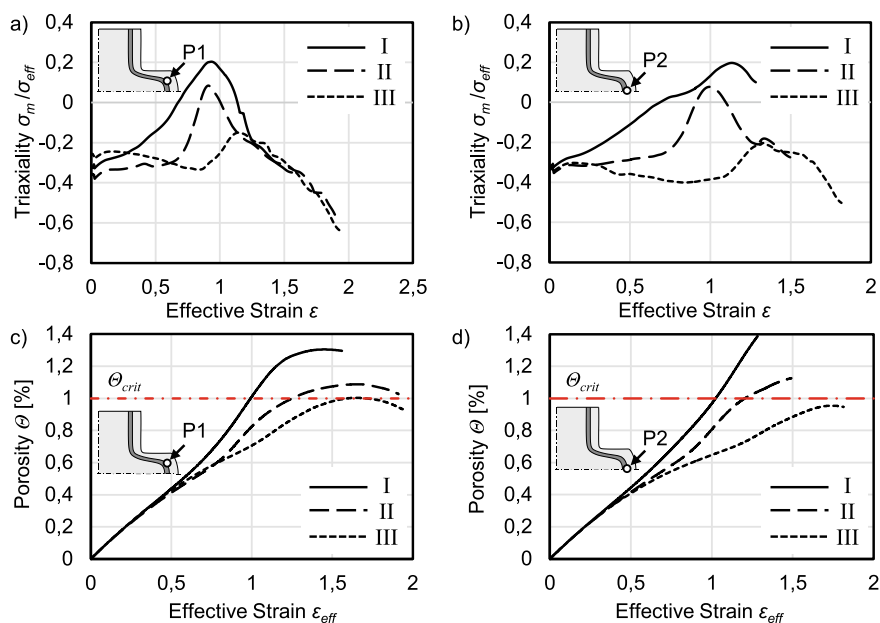


Fig. 10 Triaxiality profiles during deformation for **a** point P1 and **b** point P2 in interface and porosity for **c** P1 and **d** P2 for all geometrical variants I-III according to [11]

were manually assembled without initial bond due to clearance fit. Billets without initial bond were more likely to show several defects, such as detachment of contact surfaces, loss in stability during compression, and undesired strain localization within the reinforcing component. The formability during cold flange upsetting of extruded AA-6060/AA-7075 billets was found at least 35% higher than without bond, before delamination effects had been initiated. Two simulation approaches had been evaluated for different initial billet bonding conditions. A 3-body design with separable shear friction contact definition between joint components was suitable to model hybrid cold forging process without initial bond between the parts, for which detachment was detected by contact loss. Analysis of radial stress acting in outside shell of flange showed that increasing tensile stresses led to detachment between the components. A 1-body design with different local material properties was used for modeling of extruded billet deformation. The used porosity model approach allowed a qualitative prediction of delamination between the initially bonded billets. For quantitative estimation, further experiments should be performed in order to investigate more deeply prevailing relationships between stress triaxiality, surface enlargement during forming, and other parameters defining gained effectiveness of bond.

References

1. Estrin Y, Beygelzimer Y, Kulagin R, Gumbsch P, Fratzl P, Zhu Y, Hahn H (2021) Architecturing materials at mesoscale: some current trends. *Mater Res Lett* 9(10):399–421
2. Yoshida Y, Matsubara T, Yasui K, Ishikawa T, Sukanuma T (2012) Influence of processing parameters on bonding conditions in backward extrusion forged bonding. *Key Eng Mater* 504–506:387–392
3. Wohletz S, Groche P (2014) Temperature influence on bond formation in multi-material joining by forging. *Procedia Eng* 81:2000–2005
4. Essa K, Kacmarcik I, Hartley P, Plancak M, Vilotic D (2012) Upsetting of bi-metallic ring billets. *J Mater Process Technol* 212(4):817–824
5. Plancak M, Kacmarcik I, Vilotic D, Krsulja M (2012) Compression of bimetallic components—analytical and experimental investigation. *Int J Eng*, 157–160
6. Ossenkemper S, Dahnke C, Tekkaya AE (2019) Analytical and experimental bond strength investigation of cold forged composite shafts. *J Mater Process Technol* 264:190–199
7. Grötzinger KC, Benko K, Kotzyba P, Hering O, Liewald M, Tekkaya AE (2021) Manufacture of hybrid components with tubular reinforcement by composite hot extrusion and subsequent cold forging. In: *MEFORM*, pp 93–98
8. Kolpak F, Schulze A, Dahnke C, Tekkaya AE (2019) Predicting weld-quality in direct hot extrusion of aluminium chips. *J Mater Process Technol* 274:116294
9. Kotzyba P, Grötzinger KC, Hering O, Liewald M, Tekkaya AE (2020) Introduction of composite hot extrusion with tubular reinforcements for subsequent cold forging. In: *Proceedings of the 10th congress of the German academic association for production technology*, pp 193–201
10. Bay N (1979) Cold pressure welding—The mechanisms governing bonding. *J Manuf Sci Eng, Trans ASME* 101(2):121–127
11. Beigelzimer JE, Efros BM, Varyukhin VN, Khokhlov AV (1994) Continuum model of the structural-inhomogeneous porous body and its application for the study of stability and viscous fracture of materials deformed under pressure. *Eng Fract Mech* 48(5):629–640

Open Access This chapter is licensed under the terms of the Creative Commons Attribution 4.0 International License (<http://creativecommons.org/licenses/by/4.0/>), which permits use, sharing, adaptation, distribution and reproduction in any medium or format, as long as you give appropriate credit to the original author(s) and the source, provide a link to the Creative Commons license and indicate if changes were made.

The images or other third party material in this chapter are included in the chapter's Creative Commons license, unless indicated otherwise in a credit line to the material. If material is not included in the chapter's Creative Commons license and your intended use is not permitted by statutory regulation or exceeds the permitted use, you will need to obtain permission directly from the copyright holder.

